

Base Doping and Recombination Activity of Impurities in Crystalline Silicon Solar Cells

L. J. Geerligs^{1*}† and D. Macdonald²

¹Energy Research Centre of the Netherlands, ECN, P.O. Box 1, 1755 ZG Petten, The Netherlands

²Department of Engineering, FEIT, The Australian National University, Canberra ACT 0200, Australia

The optimisation of base doping for industrial crystalline silicon solar cells is examined with model calculations. Focus is on the relation between base doping and carrier recombination through the important impurities interstitial iron (Fe_i) and the metastable boron–oxygen (BO) complex. In p-type silicon, the optimum base resistivity is strongly dependent on defect concentration. In n-type silicon, recombination due to Fe_i is much lower and nearly independent of resistivity. Fe_i is likely representative for other transition metal impurities. In many real cells a balance between Fe_i or similar defects, and BO will occur. Copyright © 2004 John Wiley & Sons, Ltd.

KEY WORDS: silicon; base; recombination; resistivity; doping

The question of optimal base resistivity for silicon solar cell processing is of great practical interest. Decreasing base resistivity provides a way to increase V_{oc} and, accordingly, potentially the cell efficiency as well. However, it also increases Auger and radiative recombination, and reduces the effectiveness of back-surface fields (BSF), and of surface-passivating coatings. High-efficiency laboratory cells use a base resistivity of $\sim 1 \Omega \text{ cm}$, which has been empirically found to provide a good balance between these parameters. Also for industrial multicrystalline cells, a base resistivity of 1–3 $\Omega \text{ cm}$ is commonly used. Since recombination through defects and impurities in the bulk and at the surfaces of these cells is considerably higher, the question is why the optimum in this case is not found at significantly lower resistivity. Indeed, previous modelling of industrial solar cells suggests the use of a lower base resistivity. In a recent paper, Brody *et al.* describe and model the relation between the base resistivity of silicon solar cells and cell efficiency.¹ They determine the optimal base resistivity, varying parameters such as BSF, emitter resistivity, surface passivation, and cell thickness. Their general conclusion is that the optimal resistivity is lower or even much lower than the 1–3 $\Omega \text{ cm}$ currently used. For example, for 300- μm -thick cells with 20 μs bulk recombination lifetime, the optimal resistivity would be 0.24 $\Omega \text{ cm}$ in the presence of an ohmic rear contact, and 0.6 $\Omega \text{ cm}$ for a BSF.

* Correspondence to: Dr L. J. Geerligs, Energy Research Centre of the Netherlands, ECN, P.O. Box 1, 1755 ZG Petten, The Netherlands.

†E-mail: geerligs@ecn.nl

Contract/grant sponsor: NOVEM; contract/grant number: 2020.01.13.11.2002.

Contract/grant sponsor: European Commission; contract/grant number: ENK6-CT-2002-00660.

Contract/grant sponsor: Australian Research Council Discovery Program.

The paper by Brody *et al.* also suggests a tentative explanation for this discrepancy. It explains how it may be due to the presence of an (unspecified) dopant–defect interaction, which is modelled as essentially increasing the recombination activity of defects proportionally to the doping concentration N_A , without changing other recombination parameters such as energy level or ratio of capture cross-sections. One example of such a dopant–defect interaction is the boron–oxygen-related metastable defect (BO defect, for short) which strongly limits the performance of boron-doped Czochralski (Cz) wafers.² The effect of the BO defect is less important in multicrystalline wafers, because these have a lower undegraded lifetime to start with (due to other defects) and the oxygen concentration is generally lower.^{3–5}

In this paper we present another explanation for the discrepancy between modelled and empirical optimal base resistivity. This explanation is *inherent* in the relation between base resistivity and carrier recombination through impurities in the Shockley–Read–Hall (SRH) model, and is relevant for several common transition metal impurities. In the SRH model the recombination rate will either be constant or *increase* with *decreasing* base resistivity, depending on the energy level and capture cross-sections of the dominant defect. An increase in recombination rate for a decrease of the resistivity of course counteracts any beneficial effects and shifts the optimum towards higher resistivity.

The dependence of SRH recombination on resistivity is very small if the defect's capture cross-sections for holes and electrons are almost equal and its energy level is not shallow. It will be very prominent if the hole and electron capture cross-sections differ significantly and the smallest cross-section is for the majority carrier. This is the case, for example, for interstitial iron (Fe_i), one of the most dominant impurities in *p*-type multicrystalline silicon.^{6,7} Therefore we think it is probable that neglect of the relation between SRH recombination rate and base resistivity at least contributed to the discrepancy discussed above.

In this paper we will consider in detail the cases of Fe_i and, for comparison, the BO defect in industrial solar cells. Both defects drive the optimum resistivity to higher values, although via different mechanisms. It is estimated that the impact of the two defects is roughly comparable, although unfortunately the knowledge of the activity of the BO defect in multicrystalline material is limited. In addition to the effect of base resistivity, we will also shortly discuss the effect of the type (*n* or *p*) of base doping for the case of Fe_i .

The SRH recombination lifetime is, for *p*-type silicon, accurately represented by:⁸

$$\tau_{\text{SRH}} = \frac{\tau_{p0}(n_1 + \Delta n) + \tau_{n0}(N_A + p_1 + \Delta n)}{(N_A + \Delta n)} \quad (1)$$

where N_A is the base doping concentration, which is of course directly related to resistivity: a higher N_A corresponds to a lower resistivity; Δn is the excess carrier density (assumed to be equal for electrons and holes). The parameters τ_{n0} and τ_{p0} are related to the electron and hole capture cross-sections σ_n and σ_p of the recombination centre, their density N , and the carrier thermal velocities v_{th} :

$$\tau_{n0} = \frac{1}{N\sigma_n v_{\text{th},n}} \quad \text{and} \quad \tau_{p0} = \frac{1}{N\sigma_p v_{\text{th},p}}$$

The factors n_1 and p_1 are the equilibrium carrier densities when the recombination centre energy E_t coincides with the Fermi level. The thermal velocity is taken⁹ as $\sim 1.7 \times 10^7 \text{ cm s}^{-1}$.

The approximation $\Delta n \ll N_A$ is appropriate for industrial solar cells with base doping N_A larger than about 10^{15} cm^{-3} and operating at maximum power, and allows the equation to be simplified further to:

$$\tau_{\text{SRH}} = \frac{\tau_{p0}(n_1 + \Delta n) + \tau_{n0}(N_A + p_1)}{N_A} \quad (2)$$

Therefore, the lifetime will depend on the base doping concentration as:

$$\frac{\tau_{\text{SRH},1}}{\tau_{\text{SRH},2}} = \frac{N_{A,2}}{N_{A,1}} \times \frac{1 + \alpha \times (N_{A,1} + p_1)}{1 + \alpha \times (N_{A,2} + p_1)} = \frac{N_{A,2}}{N_{A,1}} \times K \quad (3)$$

where

$$\alpha = \frac{\tau_{n0}}{\tau_{p0}(n_1 + \Delta n)}$$

This means that if $N_{A,1} > N_{A,2}$, then $\tau_{SRH,1} < \tau_{SRH,2}$.

In some cases the factor K in Equation (3) will approach 1, and τ_{SRH} will be approximately linear in $1/N_A$, and as a result, approximately linear in resistivity. For example, Figure 1(a) shows the lifetime determined by a concentration of $3 \times 10^{11} \text{ cm}^{-3}$ Fe_i , as a function of base resistivity, for typical injection levels. The Fe_i recombination parameters¹⁰ are $E_c - E_t = 0.774 \text{ eV}$, $\sigma_p = 7 \times 10^{-17} \text{ cm}^2$, $\sigma_n = 5 \times 10^{-14} \text{ cm}^2$. A concentration of Fe_i around 10^{11} cm^{-3} is common in mc-Si after gettering.¹¹ The region in which the lifetime increases roughly linearly with the resistivity is clearly visible. The dependence of the lifetime on the base resistivity increases dramatically for a fixed generation rate (chosen as 0.1 suns to approximate maximum power conditions in a solar cell), rather than a fixed injection level. This striking effect is related to the dependence of SRH recombination on injection level. Figure 1(a) clearly shows that a significant concentration of Fe_i will result in a preference for higher base resistivity, necessary to maintain a reasonable carrier lifetime.

Figure 1(b) shows a similar lifetime calculation for the BO defect. The BO defect in multicrystalline silicon has been studied in several papers.^{3–5} Because absolute capture cross-sections of this defect are not known, the relation between defect density and degradation of lifetime (from τ_i to τ_f) is expressed through a ‘normalized defect density’ N_t^* :

$$N_t^* \equiv \frac{1}{\tau_f} - \frac{1}{\tau_i}$$

N_t^* is proportional to the boron concentration, therefore N_t^*/N_A (in $10^{16} \text{ cm}^3 \mu\text{s}^{-1}$) can be used to remove the dependence on the boron concentration.

The reported N_t^*/N_A varies from less than $0.01 \times 10^{16} \text{ cm}^3 \mu\text{s}^{-1}$ for 6 ppm oxygen, to $0.2 \times 10^{16} \text{ cm}^3 \mu\text{s}^{-1}$ for 20 ppm. The oxygen concentration in multicrystalline ingots typically is between 10–20 ppm in the bottom, decreasing to less than 5 ppm in the top.¹² The value of $N_t^*/N_A = 0.01 \times 10^{16} \text{ cm}^3 \mu\text{s}^{-1}$ is therefore a representative value, and is used in Figure 1(b). In this case the the majority of the dependence of lifetime on resistivity arises from the chemical presence of boron in the defect itself, and not from the electronic properties of the defect. The increase of lifetime with resistivity is slightly stronger than linear because the BO defect has an asymmetry of capture cross-sections¹³ of a factor 9.3.

Figure 1 shows that the impact of both defects is similar for realistic defect densities. Clearly the balance will depend on the exact defect concentrations present in a particular material. For a precise analysis of their relative importance in multicrystalline material, the relation between N_t^* , oxygen concentration, and other material parameters would have to be known in more detail. Also, the Fe_i concentration in cells can vary rather strongly with process steps and process parameters.

We note that the Auger and radiative recombination lifetime¹⁴ are much higher than the SRH lifetime in Figure 1, for resistivity higher than about $0.05 \Omega \text{ cm}$. Only for resistivity below $0.035 \Omega \text{ cm}$ is the recombination rate from these processes higher than the SRH rate.

To illustrate how the dependence of lifetime on base resistivity can affect solar cells, Figure 2 shows the calculated cell efficiency as a function of base resistivity. The cells were modelled with parameters typical for industrial processing, with a screen-printed Al-BSF modelled as a 9- μm -thick region of high acceptor concentration ($4 \times 10^{18} \text{ cm}^{-3}$) and low lifetime.¹⁵ The calculations were performed in PC1D.¹⁶ Three cases are compared: (i) Fe_i recombination centres with a concentration of 10^{11} cm^{-3} ; (ii) BO centres with $N_t^*/N_A = 0.01 \times 10^{16} \text{ cm}^3 \mu\text{s}^{-1}$; and (iii) mid-gap recombination centres with $\sigma_n = \sigma_p$ and $\tau_{SRH} \simeq 20 \mu\text{s}$ (at $1.5 \Omega \text{ cm}$, only weakly dependent on base resistivity).

From plots like Figure 2, for a range of defect concentrations, the optimal base resistivity as a function of defect concentration can be derived. The results are given in Figure 3. Clearly, a higher Fe_i or BO concentration leads to a *higher* optimal base resistivity. Also shown, in Figure 3(b), is that, in contrast, for mid-gap

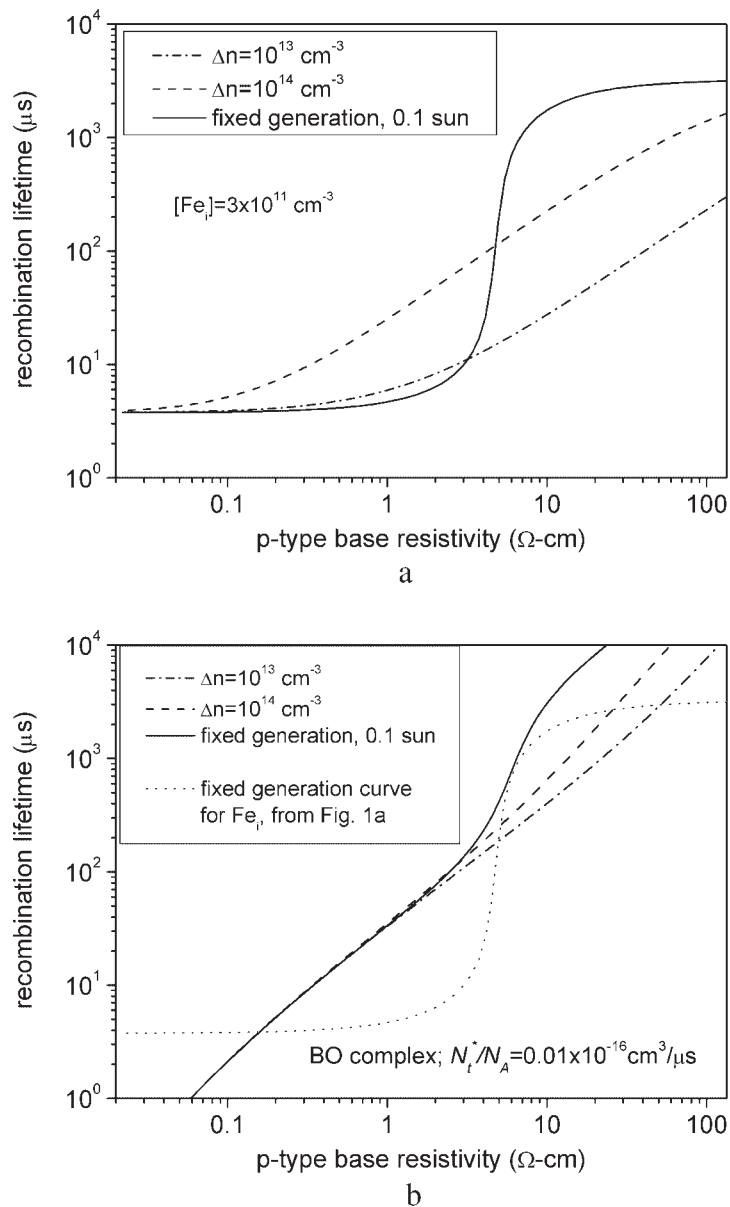


Figure 1. Lifetime calculated as a function of base resistivity: (a) for a concentration of $3 \times 10^{11} \text{ cm}^{-3}$ Fe_i impurities, according to Equation (1). For a fixed generation of 0.1 sun, the dependence on base resistivity is even stronger than for a fixed injection level. Base resistivity was related to dopant concentration N_A using PC1D; (b) for the BO defect with normalized defect density $N_t^*/N_A = 0.01 \times 10^{-16} \text{ cm}^3/\mu\text{s}$ at $\Delta n = 10^{15} \text{ cm}^{-3}$. For reference, a dotted line reproduces the 0.1 sun curve for Fe_i from (a)

recombination centers with $\sigma_n = \sigma_p$, where the bulk lifetime depends only weakly on base resistivity, a higher defect concentration leads to a *lower* optimal base resistivity.

It can be noted from Figure 1 that recombination *only* due to Fe_i or BO leads to very high lifetime values for high base resistivity. Therefore this modelling results in rather high optimal resistivity values of 10 $\Omega\text{ cm}$ and higher. It is likely that in reality other impurities and defects will impose a cap on the actual bulk lifetime. The results of imposing such a lifetime cap in the modelling are also shown in Figures 2 and 3. A cap does not change the qualitative behaviour of the dependence of optimal base resistivity on defect concentration in Figure 3, but it

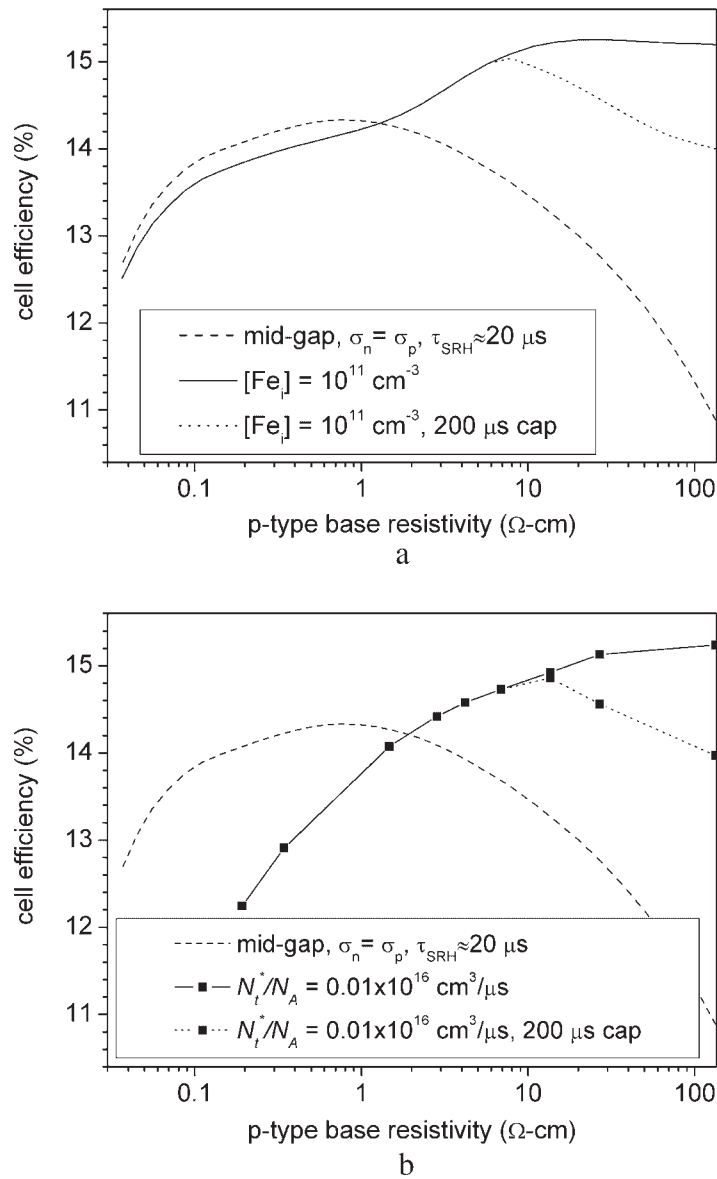


Figure 2. Cell efficiency calculated with PCID as a function of base resistivity: (a) for recombination via $10^{11} \text{ cm}^{-3} \text{ Fe}_i$ impurities, and for comparison, for recombination via mid-gap defects with $\sigma_n = \sigma_p$ and $\tau_{\text{SRH}} \approx 20 \mu\text{s}$ at $1.5 \Omega \text{ cm}$, weakly dependent on resistivity; (b) for the BO defect with normalized defect density $N_t^*/N_A = 0.01 \times 10^{-16} \text{ cm}^3/\mu\text{s}$ at $\Delta n = 10^{15} \text{ cm}^{-3}$. An industrial cell process with Al-BSF rear-surface passivation is modeled. The dotted line represents cell efficiency assuming a cap of $200 \mu\text{s}$ on the bulk lifetime

shifts the curve to lower values of optimal resistivity. In both cases, a relatively low cap of $20 \mu\text{s}$ can result in an optimum below $1 \Omega \text{ cm}$. The position of the curves is influenced by the exact defect parameters, especially the energy level of the defect. The curves are rather independent of the model for the solar cell, except that if the model does not include rear-surface passivation (such as the presence of a back surface field) there is no significant dependence of cell efficiency on bulk lifetime.

The behaviour described above for Fe_i is due to the fact that the hole capture cross-section is much smaller than the electron capture cross-section. Because of the small hole capture cross-section, even though holes are

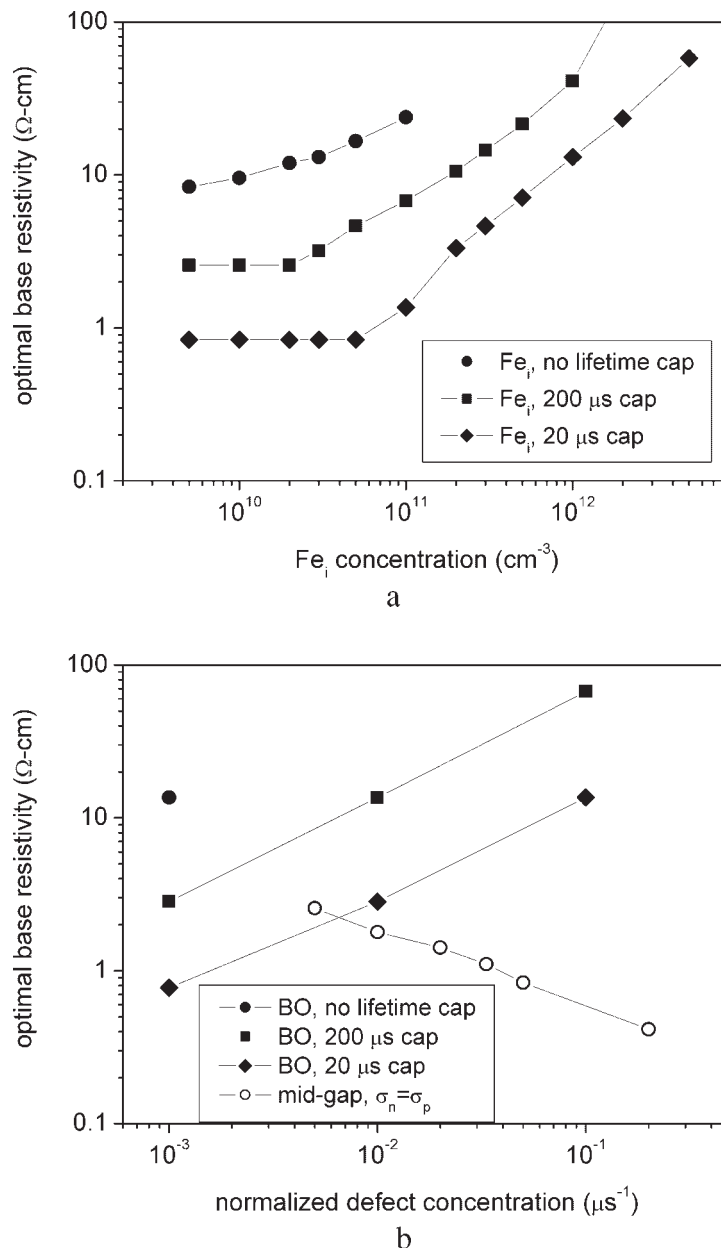


Figure 3. (a) Optimal base resistivity calculated as a function of Fe_i concentration, for cells as in Figure 2; (b) optimal base resistivity calculated as a function of BO complex concentration, for cells as in Figure 2. As a reference, also shown is the optimal doping as a function of defect concentration, for a mid-gap defect with $\sigma_n = \sigma_p$. Defect densities are represented as normalized values, i.e., as N_i^* at $N_A = 10^{16} \text{ cm}^{-3}$ for the BO complex, and as $1/\tau$ for the mid-gap defect. The results are shown for modelling without bulk lifetime cap, and for caps of 200 and 20 μs

majority carriers, their capture rate is limiting the recombination rate. This capture rate is proportional to the concentration of holes, which is in turn determined by the base doping.

If holes are the minority carrier their concentration will be determined by the injection level, and not by the base doping. In that case, a small hole capture cross-section will result in a low recombination rate (high lifetime) *virtually independent* of resistivity. To illustrate this, Figure 4 shows the lifetime in p -type and n -type

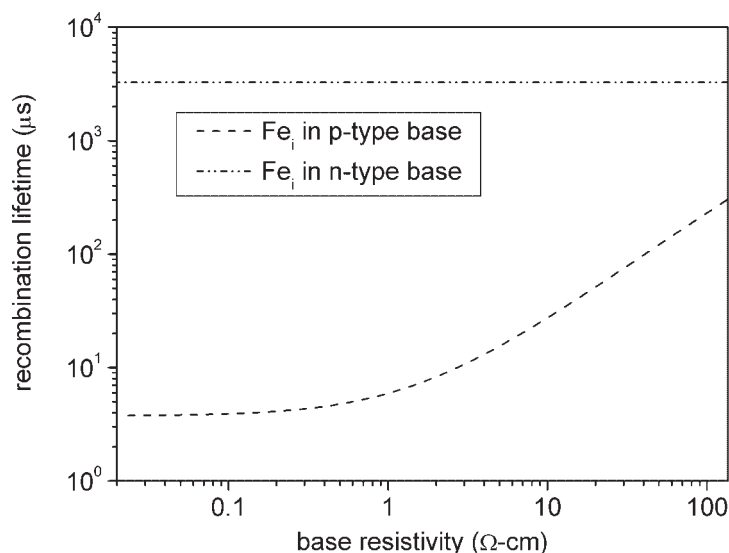


Figure 4. Minority-carrier lifetime calculated as a function of base resistivity in n - and p -type silicon, for a concentration of $3 \times 10^{11} \text{ cm}^{-3}$ of Fe_i . The calculations are for an injection level of $\Delta n = 10^{13} \text{ cm}^{-3}$

silicon, both with $3 \times 10^{11} \text{ cm}^{-3}$ Fe_i impurities. The difference in lifetime between the two substrates is several orders of magnitude. Since Fe_i may be expected to be a dominant impurity in n -type silicon, too, this may explain the unusually high lifetimes recently observed in n -type silicon.¹⁷

It is important to note that Fe is representative for a wider range of impurities. The effects described in this paper are intrinsic properties of deep SRH centres with smaller cross-sections for majority carriers than minority carriers. Many other transition metal contaminants in silicon have capture cross-sections with asymmetry similar to Fe_i .¹⁹

In conclusion, asymmetrical capture cross-sections of impurities, for electrons larger than for holes, provide an explanation for the empirical preference for higher resistivities in p -type solar grade silicon than might otherwise be expected. It is also an explanation for remarkably high carrier lifetimes in n -type solar grade silicon. The physics of this effect is fundamentally different from and independent of chemical dopant–defect interactions such as occur with the BO defect. When impurities in silicon wafers are reduced (including the oxygen content), the optimal bulk resistivity may shift downwards, as indicated in Figure 3. The concentration of (active) defects can be reduced by, for example, improved silicon feedstock, improved ingot growth technology, improved gettering, or by hydrogen passivation. Therefore, the optimal resistivity determined empirically several years ago may have changed for the present wafer and cell production technologies.

Acknowledgements

The authors acknowledge the support of the Netherlands Agency for Energy and the Environment (NOVEM), contract 2020.01.13.11.2002, the European Commission, contract ENK6-CT-2002-00660 and the Australian Research Council through the Discovery Program.

REFERENCES

1. Brody J, Rohatgi A, Yelundur V. Bulk resistivity optimization for low-bulk-lifetime silicon solar cells. *Progress in Photovoltaics: Research and Applications* 2001; **9**(4): 273–285.
2. Bothe K, Schmidt J, Hezel R. Comprehensive analysis of the impact of boron and oxygen on the metastable defect in Cz-silicon. *Proceeding of the 3rd World Conference on Photovoltaic Energy Conversion*, Osaka, Japan, 11–18 May 2003; 927–930.

3. Dhamrin M, Akihide T, Hashigami H, Saitoh T. Light-induced lifetime degradation of commercial multicrystalline silicon wafers. *Proceedings of the 29th IEEE Photovoltaic Specialists Conference* 2002; 395–398.
4. Damiani BM. Light induced degradation in promising multi-crystalline silicon materials and cells. *Proceedings of the 3rd World Conference on Photovoltaic Energy Conversion*, Osaka, Japan, 11–13 May, 2003; 927–930.
5. Macdonald DH, Geerligs LJ, Riepe S. Light-induced lifetime degradation in multicrystalline silicon. *13th Workshop on Crystalline Silicon Solar Cell Materials and Processes. Extended Papers and Abstracts*. NREL: Golden, 2002; 182–285.
6. Sopori BL, Jastrzebski L, Tan T. A comparison of gettering in single- and multicrystalline silicon for solar cells. *Proceedings of the 25th IEEE Photovoltaic Specialists Conference* 1996; 119–122.
7. Geerligs LJ. Impact of defect distribution and impurities on multicrystalline silicon solar cell efficiency. *Proceedings of the 3rd World Conference on Photovoltaic Energy Conversion*, Osaka, Japan, 11–13 May 2003; 1044–1047.
8. Blakemore JS. *Semiconductor Statistics. International Series of Monographs on Semiconductors*, Vol. 3. Pergamon Press: Oxford, 1962.
9. Samudra G *et al.* High-field electron transport for ellipsoidal multivalley band structure of silicon. *Journal of Applied Physics* 1992; **72**(10): 4700–4704.
10. Istratov A, Hieslmair H, Weber ER. *Applied Physics* 1999; **A 69**: 13. Macdonald D, Cuevas A, Wong-Leung J. *Journal of Applied Physics* 2001; **89**(12): 7932.
11. Ballif C *et al.* Lifetime investigations of degradation effects in processed multicrystalline silicon wafers. *Proceedings of the 17th European Photovoltaic Solar Energy Conference*, Munich, 2002; 1818–1821. Geerligs LJ. Multicrystalline silicon: relation between ingot quality and cell efficiency. *12th Workshop on Crystalline Silicon Solar Cell Materials and Processes. Extended Papers and Abstracts*. NREL: Golden, 2002; 288–292.
12. Schönecker A, Geerligs LJ, Müller A. Casting technologies for solar silicon wafers: block casting and ribbon-growth-on substrate. *Solid State Phenomena* 2004; **95–96**: 149–158.
13. Rein S, Glunz SW. Electronic properties of the metastable defect in boron-doped Czochralski silicon: unambiguous determination by advanced lifetime spectroscopy. *Applied Physics Letters* 2003; **82**: 1054–1056.
14. Kerr MJ, Cuevas A. *Journal of Applied Physics* 2002; **91**: 2473.
15. Tool CJJ *et al.* Influence of wafer thickness on the performance of multicrystalline Si solar cells: an experimental study. *Progress in Photovoltaics: Research and Applications* 2001; **10**: 279–291. In the present paper, a higher diffusion length in the BSF— $L_D = 4.5 \mu\text{m}$ —is used because this fits the experimental internal quantum efficiency curves better.
16. Basore P, Clugston DA. *PCID v.5.5*. University of New South Wales, 2000.
17. Cuevas A *et al.* Millisecond minority carrier lifetimes in *n*-type multicrystalline silicon. *Applied Physics Letters* 2002; **81**(26): 4952–4954.
18. Libal J *et al.* Properties of *n*-type multicrystalline silicon: lifetime, gettering and H-passivation. Accepted for presentation at the 19th European Photovoltaic Solar Energy Conference, Paris, 7–11 June 2004.
19. Macdonald DH, Geerligs LJ. *Recombination Activity of Iron and Other Transition Metals in *p*- and *n*-type Crystalline Silicon*. Accepted for presentation at the 19th European Photovoltaic Solar Energy Conference, Paris, 7–11 June 2004.